

Dynamics of trehalose molecules in confined solutions

Gérald Lelong

Centre de Recherche sur la Matière Divisée, 45071 Orleans Cedex 2, France

David L. Price

Centre de Recherche sur les Matériaux à Haute Température, 45071 Orleans Cedex 2, France

John W. Brady

Department of Food Sciences, Cornell University, Ithaca, New York 14853

Marie-Louise Saboungi^{a)}

Centre de Recherche sur la Matière Divisée, 45071 Orleans Cedex 2, France

(Received 22 January 2007; accepted 8 June 2007; published online 14 August 2007)

The dynamics of trehalose molecules in aqueous solutions confined in silica gel have been studied by quasielastic neutron scattering (QENS). Small-angle neutron scattering measurements confirmed the absence of both sugar clustering and matrix deformation of the gels, indicating that the results obtained are representative of homogeneous trehalose solutions confined in a uniform matrix. The pore size in the gel is estimated to be 18 nm, comparable to the distances in cell membranes. For the QENS measurements, the gel was prepared from D₂O in order to accentuate the scattering from the trehalose. Values for the translational diffusion constant and effective jump distance were derived from model fits to the scattering function. Comparison with QENS and NMR results in the literature for bulk trehalose shows that confinement on a length scale of 18 nm has no significant effect on the translational diffusion of trehalose molecules. © 2007 American Institute of Physics.

[DOI: [10.1063/1.2753841](https://doi.org/10.1063/1.2753841)]

INTRODUCTION

The nonreducing disaccharide trehalose is produced in large quantities under conditions of water stress in a number of cold- and drought-adapted organisms. A particular example is the plant species *Selaginella lepidophylla*, more commonly called Rose of Jericho, which is extraordinarily resistant to drought. These flowering plants look quite dead after dehydration in which state they can survive for long periods, after which they recover fully with the first traces of water. For this reason, they are called “*resurrection plants*.”¹ The presence of trehalose in these organisms is known to be responsible for their desiccation tolerance, but the mechanisms of its activity are incompletely understood. Two types of process have been proposed:

- During dehydration, the interactions between hydration water and membranes are progressively replaced by new interactions between the sugar molecules and the head groups of the lipids. Among sugars, trehalose is the most efficient in the water replacement² and acts as a bridge between lipids, preventing any collapse.³
- Because they have a high glass transition temperature ($T_g \approx 393$ K) (Refs. 4 and 5) compared with other mono- and disaccharides, trehalose solutions can vitrify at room temperature in the intermembrane space, stabilizing the proteins and maintaining the integrity of the cellular structure.^{6,7}

Both hypotheses take molecular dynamics into consideration. Köper *et al.*,⁸ Branca *et al.*,⁹ and Ekdawi-Sever *et al.*¹⁰ have studied dynamics of both trehalose and water molecules as a function of sugar concentration and temperature. As in other sugar solutions, in particular those with the monomeric component D-glucose, the dynamics of both trehalose and water molecules are very sensitive to the concentration of solutes. For example, the translational diffusion rate of trehalose molecules at room temperature is reduced by a factor of 300 and that of water molecules by a factor of 30, for sugar concentrations going from 16 to 71 wt %.¹⁰ These bulk measurements provide important information on the dynamics of the solute, but are not adequate to understand what happens in real systems where the effects of confinement on the nanometer scale have to be taken into account. It is therefore necessary to study the dynamics of these solutes in a confined region with length scales that mimic those found in living cells.

Recently, we reported a quasielastic neutron scattering (QENS) experiment on the molecular dynamics of D-glucose solutions confined in an aqueous silica gel.¹¹ The sol-gel process is an original and interesting way to investigate the dynamics of confined molecules without the complication of dynamics of nonconfined molecules. Complemented with small-angle neutron scattering (SANS) measurements, our study showed that, for an average pore diameter around 18–20 nm, the dynamics of D-glucose molecules at room temperature are not significantly affected by steric effects in comparison with bulk solutions of the same concentrations.^{12,13} We did, however, observe an increase in the SANS intensity at low Q that suggested the possibility of

^{a)} Author to whom correspondence should be addressed. Electronic mail: mls@cnsr-orleans.fr

TABLE I. Summary table of the samples measured: sugar type, notation, composition, and the measurements carried out.

Sugar	Name	Molar ratios	Experiment
Glucose	A3	TEOS (7.2)-D ₂ O (1110)-urea (1.6)-HNO ₃ (0.025)-C ₆ H ₇ D ₅ O ₆ (55.5)	SANS
Trehalose	AT1	TEOS (7.2)-D ₂ O (1110)-urea (1.6)-HNO ₃ (0.025)-C ₁₂ H ₁₃ D ₉ O ₁₁ (0)	QENS
	AT2	TEOS (7.2)-D ₂ O (1110)-urea (1.6)-HNO ₃ (0.025)-C ₁₂ H ₁₃ D ₉ O ₁₁ (10.6)	QENS
	AT3	TEOS (7.2)-D ₂ O (1110)-urea (1.6)-HNO ₃ (0.025)-C ₁₂ H ₁₃ D ₉ O ₁₁ (29.3)	QENS and SANS

an aggregation of the sugar molecules or of a deformation of the silica matrix leading to the formation of larger pores.¹¹ In this paper, we report a QENS study of trehalose solutions confined in aqueous silica gels to see if the dynamics of these molecules are affected by the confinement. In addition, we have carried out new SANS measurements on both glucose and trehalose solutions confined in silica gels using the contrast variation method, in order to investigate the possibility of aggregation and/or matrix deformation suggested by our previous results.¹¹

SYNTHESIS

Aqueous silica gels were synthesized by a sol-gel process¹⁴ used previously for the confinement of glucose solutions.¹¹ The gels had the molar ratios tetraethylorthosilicate TEOS:water:urea:HNO₃=7.2:1110:1.6:0.025. D-glucose and α -*trehalose* contain hydrogen atoms directly bounded to an oxygen atom. In order to avoid their exchange with the solvent deuterons, sugar was first mixed with a large excess of heavy water to replace the exchangeable hydrogen atoms by deuterium, yielding partially deuterated glucose (C₆H₇D₅O₆) and trehalose (C₁₂H₁₄D₈O₁₁). These sugars were dried and used to prepare the gels.

The confined sugar solutions had the following molar ratios: TEOS:D₂O:urea:HNO₃:sugar = 7.2:1110:1.6:0.025:*x*, with *x*=55.5 for glucose and *x*=0, 10.6, and 29.3 for trehalose. These concentrations would correspond to 30 wt % of glucose and 0, 13.4, and 30 wt % of trehalose in fully protonated solutions, or 31.6, 0, 14.2, and 31.6 wt % taking only the sugar and water into account. The four gels will be denoted as A3 (30 wt % of glucose), AT1 (pure gel without sugar), AT2 (13.4 wt % of trehalose), and AT3 (30 wt % of trehalose), respectively. The notations, compositions, and measurements carried out in this study are summarized in Table I. All the samples obtained were optically clear, implying a complete absence of phase separation.

EXPERIMENTS

For the SANS experiments, samples 1 or 2 mm thick were sandwiched between two quartz windows. The measurements were conducted on the NG-7 30 m SANS instrument¹⁵ at the NIST Center for Neutron Research (NCNR) reactor at an incident wavelength of 6 Å. Detector distances of 1, 4, and 13 m were used sequentially to cover a large range of *Q* (0.0035–0.47 Å⁻¹). The two-dimensional patterns were corrected for background and empty-cell scattering and finally radially averaged using the data reduction software developed at NCNR.¹⁶

The QENS experiments were carried out on the IRIS backscattering spectrometer at the pulsed spallation source ISIS of the Rutherford Appleton Laboratory.¹⁷ The samples were loaded into annular aluminum cans with an annular spacing of 0.4 mm, sealed, and placed within the radiation shield of a closed-cycle refrigerator in which the temperature could be controlled to ± 1 K. The experiments were carried out at an incident wavelength of 6.7 Å, so that the wave vector transfer *Q* (for elastic scattering) covered the range of 0.46–1.84 Å⁻¹. Samples were measured at 270, 300, and 330 K with run times of approximately 6 h. The energy resolution and intensity normalization were determined from a measurement with a vanadium hollow cylinder in the same conditions as those used for the sample measurements; the resolution was found to be 17.5 μ eV with the analyzer crystals in the PG002 configuration (002 reflection of pyrolytic graphite). The QENS spectra were corrected for container scattering and background and the scattering functions *S(Q, E)* were obtained, where *E* is the energy transfer. Data sets were reduced and analyzed with the standard analysis package MODES.¹⁸

RESULTS: STRUCTURE

We used the contrast variation method to extract the signals from the different constituents of the samples. SANS is sensitive to fluctuations in scattering length density (SLD) present in the sample. Since the SLD of H₂O ($\rho_{\text{H}_2\text{O}} = -5 \times 10^{-7}$ Å⁻²) and D₂O ($\rho_{\text{D}_2\text{O}} = 6.36 \times 10^{-6}$ Å⁻²) have opposite signs, it is possible by using different H₂O/D₂O ratios to mask the scattering from the silica network, or that from the sugar molecules, in order to reveal any inhomogeneities in the distribution of sugar molecules that may be present.

We first studied confined solutions of glucose to investigate the possibility of aggregation and/or matrix segregation suggested by our earlier results.¹¹ The first step was to determine the SLD of each constituent of the sample. The SLD of the silica matrix was determined by measuring six aqueous silica gels with H₂O/D₂O volume percentages of 100/0, 80/20, 60/40, 40/60, 20/80, and 0/100. Figure 1 shows a log-log plot of the SANS data for these gels without sugar. An extinction of the scattering signal occurs around a volume fraction H₂O/D₂O=40/60. Since the scattering intensity *I(Q)* is proportional to the square of the amplitude *A(Q)*, which is itself proportional to the SLD, the contrast match point can be determined precisely by plotting the square root of intensity versus volume fraction of H₂O (Fig. 2) and is found to be 38 \pm 1%, corresponding to an SLD $\rho_{\text{SiO}_2} = 3.8 \times 10^{-6}$ Å⁻². The SLD of D-glucose molecules alone (C₆D₅H₇O₆) and of a 30 wt % D₂O solution (as in sample

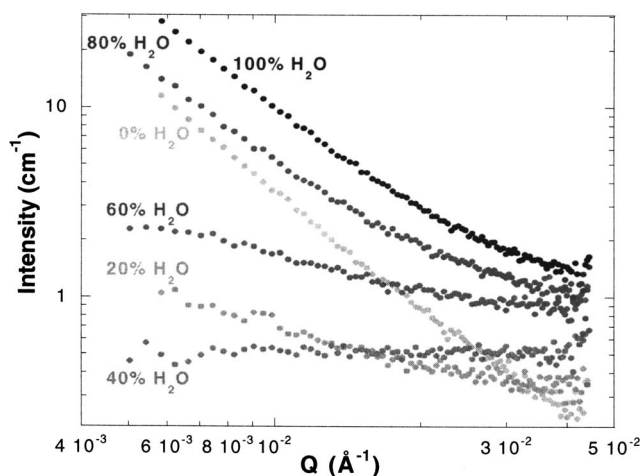


FIG. 1. SANS spectra for silica gel samples for different volume percentages of H_2O .

A3) have been calculated to be 4.15×10^{-6} and $5.86 \times 10^{-6} \text{ \AA}^{-2}$, respectively. Different H_2O/D_2O ratios were used to observe (i) the silica matrix, with SLD ($43 H_2O/57 D_2O$)=SLD (sugar) and (ii) the distribution of sugar molecules, with SLD ($38 H_2O/62 D_2O$)=SLD (SiO_2). In addition (iii), a test sample with a uniform SLD, SLD ($43 H_2O/57 D_2O$ /sugar)=SLD (SiO_2), has also been synthesized. These three samples will be denoted as gel-silica, gel-glucose, and gel-test, respectively. Log-log plots of the scattering intensity of the three samples are shown in Fig. 3. As expected, the test sample presents a flat profile, confirming both the homogeneity in the SLD of the gel and the validity of our calculations and synthesis. The measured intensity is due only to an incoherent background produced principally by the hydrogen atoms present in the water and glucose molecules. For the gel-sugar sample, a similar flat scattering profile is observed, indicating that there is no sugar clustering or concentration gradient on the SANS length scale (3–100 nm) in these gels. The spectrum of the

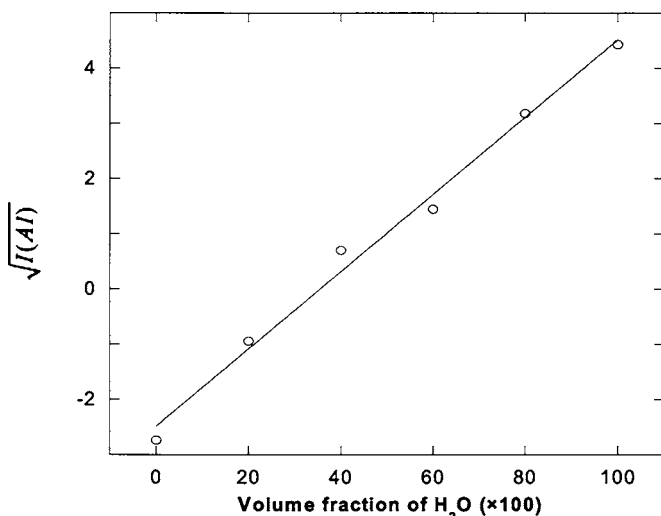


FIG. 2. Square root of the intensity at $Q=0.007 \text{ \AA}^{-1}$ as a function of volume fraction of H_2O . The contrast matching point of the silica is determined to be $38 \pm 1\%$, corresponding to a scattering length density $\rho_{SiO_2}=3.8 \times 10^{-6} \text{ \AA}^{-2}$.

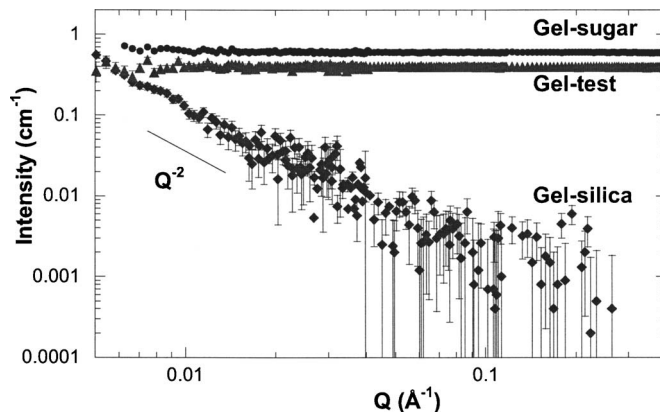


FIG. 3. SANS spectra for silica gels containing 30 wt % of glucose (A3). The three samples gel-sugar (circles), gel-silica (diamonds), and gel-test (triangles) represent the scattering from the different components of the silica gel A3. The Q^{-2} line is a guide for the eye.

gel-silica sample shows a Q^{-2} power law, typical of a fractal structure,¹⁹ but no additional increase in scattering intensity at low Q . The increased scattering observed at low Q in our previous work¹¹ is thus due neither to the formation of large pores in the silica matrix nor to sugar clustering.

Schaefer and Keefer¹⁹ studied the variation of the small-angle x-ray scattering profile with gelation time in silica gels. They found that for an incompletely gelled sol the scattering intensity showed an increased scattering with a Q^{-4} dependence at low Q values, similar to that reported in Ref. 11, which indicates the presence of a marked interface between two homogenous media. We tested the possibility of incomplete gelation in our samples by measuring a gel containing glucose (A3) at different times in the gelation process (Fig. 4). An increase in scattering at low Q observed for shorter gelation times (15 h) disappeared after a longer time (20 h), leaving the Q^{-2} power law component. It appears that the addition of sugar molecules during the synthesis slows down

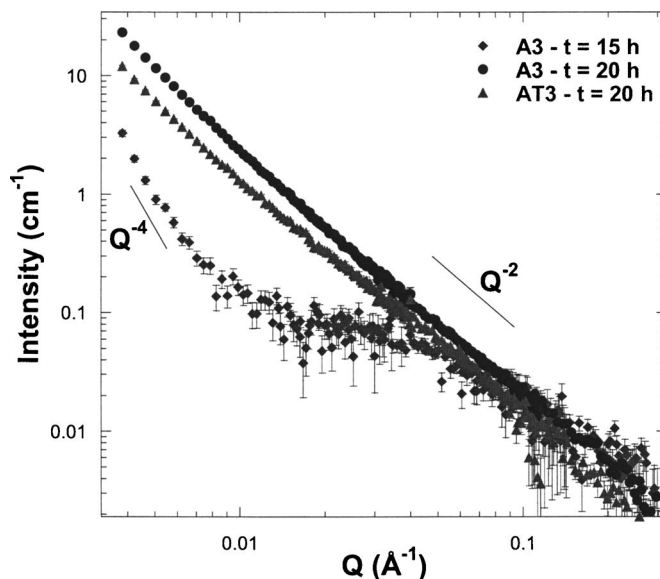


FIG. 4. SANS spectra for gels containing 30 wt % of glucose (A3) at different gelation times and for a gel containing 30 wt % of trehalose (AT3). The Q^{-2} and Q^{-4} lines are a guide for the eye.

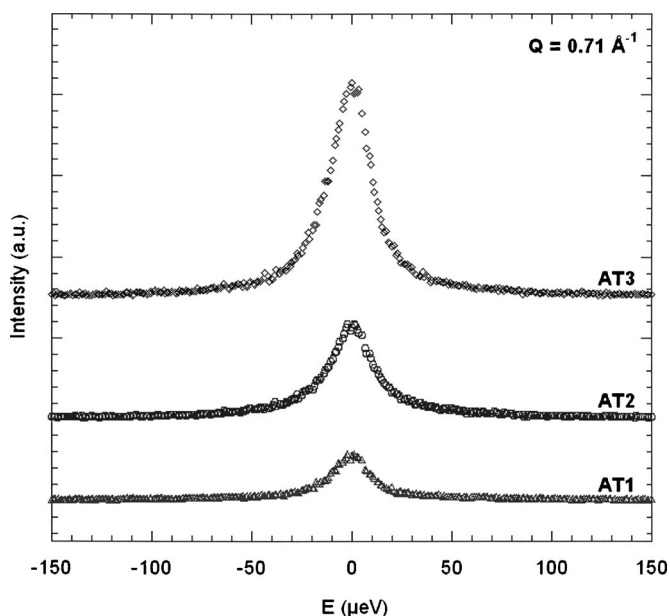


FIG. 5. QENS spectra at $Q=0.71 \text{ \AA}^{-1}$ for the pure gel AT1 and gels with confined trehalose solutions AT2 and AT3, all at 300 K.

the polycondensation rate and requires a longer gelation time. Figure 4 also shows the corresponding result for a gel containing trehalose (AT3) after 20 h of gelation time, showing that the gelation was complete for this sample also. After a correct aging, the gels with sugar, either glucose or trehalose, are identical to those without sugar from a structural point of view, meaning that our previous estimate¹¹ of a pore size of 18–20 nm is still valid. All QENS measurements were carried out on samples completely gelled, i.e., after more than 20 h of aging.

RESULTS: DYNAMICS

QENS measurements were carried out on the pure gel sample (AT1) and the two confined trehalose solutions (AT2 and AT3). The scattering function $S(Q, E)$ was fitted with a combination of theoretical functions convolved with the resolution of the instrument. The best fit was obtained with a combination of one delta function, one or two Lorentzians $L_n(W_n, E)$ depending on the concentration and/or the temperature, and a sloping background. The signal coming from the trehalose was extracted by subtracting the pure gel AT1 from the gels with sugar (AT2 and AT3) and will be denoted as AT2-AT1 and AT3-AT1. To take into account the different attenuation by the pure gel and the gel containing sugar, the scattering for the pure gel was multiplied by the attenuation factor for the trehalose prior to the subtraction. The validity of this procedure rests, of course, on the assumption that the effect of the trehalose on the dynamics of the gel host is negligible. This is supported by the fact that the gel is deuterated and contributes relatively little to the total scattering, as shown below.

Typical spectra obtained at 300 K are shown in Fig. 5. The effect of the trehalose concentration on the full width at half maximum is clearly seen, indicating a slowing down of the diffusive motions of sugar molecules. Translational dynamics information can be extracted from the Q^2 dependence

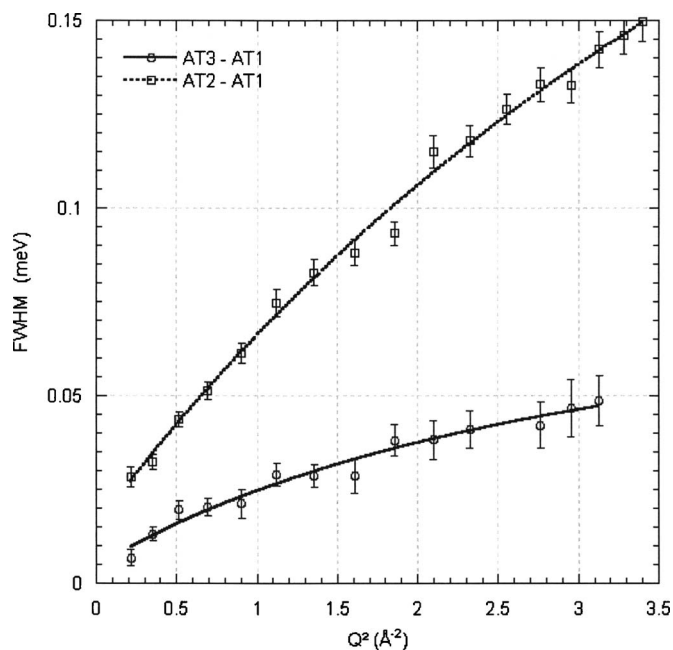


FIG. 6. Full width at half maximum of the narrower Lorentzian fitted to the QENS spectra for the confined trehalose at 300 K. The lines represent least-squares fits described in the text.

of W_1 , the full width at half maximum of the narrower Lorentzian, which can be least-squares fitted by the following expression used in previous studies on bulk and confined sugar solutions:^{11–13}

$$W_1 = \alpha_1 + \frac{\beta_1 Q^2}{(1 + \gamma_1 Q^2)}. \quad (1)$$

The fits of narrower Lorentzians are shown as continuous lines in Fig. 6 and the values of the parameters are presented in Table II.

According to the model of Teixeira *et al.*²⁰ and used in our previous studies,^{11–13} the translational diffusion constant D and an effective jump distance l can be extracted from the parameters β_1 and γ_1 associated with the rapid jump diffusion model:

$$\beta_1 = 2\hbar D, \quad (2a)$$

$$\gamma_1 = \frac{l^2}{6}. \quad (2b)$$

The fitted values of D and l are shown in Table III.

Figure 7 shows a comparative plot of our study on confined trehalose solution with other results found in the literature. At 300 K, the diffusion rate of confined trehalose molecules decreases from 0.44×10^{-5} to $0.2 \times 10^{-5} \text{ cm}^2 \text{ s}^{-1}$ for sugar concentrations going from 13.4 to 30 wt %, respectively. Branca *et al.*⁹ observed by NMR a diffusion rate of 0.37×10^{-5} and $0.22 \times 10^{-5} \text{ cm}^2 \text{ s}^{-1}$ for 14 and 30 wt % trehalose bulk solutions. Similar values were found by Ekdawisever *et al.*¹⁰ with 0.42×10^{-5} and $0.14 \times 10^{-5} \text{ cm}^2 \text{ s}^{-1}$ for trehalose solutions of 16 and 28 wt %, and values of 0.19×10^{-5} and $0.16 \times 10^{-5} \text{ cm}^2 \text{ s}^{-1}$ for sucrose solutions of same concentrations. QENS experiments carried out by Köper *et al.*⁸ indicated a diffusion rate of $0.22 \times 10^{-5} \text{ cm}^2 \text{ s}^{-1}$ for a

TABLE II. Parameters fitted to the full width at half maximum of the narrower Lorentzian line for different temperatures and samples.

			α_1 (meV)	β_1 (meV \AA^2)	γ_1 (\AA^2)
270 K	AT2	13.4 wt %	0.003 ± 0.005	0.03 ± 0.01	0.01 ± 0.29
300 K	AT1	0 wt %	-0.02 ± 0.02	0.32 ± 0.05	0.25 ± 0.07
	AT2	13.4 wt %	0.020 ± 0.008	0.10 ± 0.02	0.21 ± 0.07
	AT3	30 wt %	0.005 ± 0.003	0.032 ± 0.007	0.4 ± 0.1
	AT2-AT1	13.4 wt %	0.015 ± 0.003	0.058 ± 0.005	0.14 ± 0.04
	AT3-AT1	30 wt %	0.004 ± 0.003	0.026 ± 0.007	0.3 ± 0.1
330 K	AT2	13.4 wt %	0.03 ± 0.01	0.12 ± 0.02	0.09 ± 0.05

30 wt % trehalose solution at 300 K. Comparing these results with those of the Table III, we find that no significant change in the translational diffusion rate is observed with a confinement of 18 nm.

DISCUSSION

The lack of any observable effect of confinement on the scale of 18 nm, also seen in our previous work on D-glucose solutions, shows that the confinement effect is really weak at this length scale. This result is probably due to the significant difference between the average pore size and the diameter of the sugar molecule, and is in good agreement with preliminary MD simulations of the same system. Adding the first hydration sphere, the diameter of a trehalose molecule can be estimated at 12–13 \AA , a value 15 times lower than the average pore diameter. Considering that an additional water shell will add a further amount of 5–8 \AA , and that, in low concentration solution, the number of water molecules per trehalose is enough for at least two to three hydration spheres, it is not surprising that the sugar dynamics are not significantly affected by the presence of the silica walls. Nevertheless, the conclusion that, on this length scale, the confined solute dynamics are equivalent to the dynamics of the same solute without confinement is significant, both for molecular dynamics simulations and for the studies of protein-sugar-water systems, where sugar molecules at the surface of the proteins are considered to be confined.

TABLE III. Physical constants calculated from the fits to the full width at half maximum of the narrower Lorentzian as a function of Q^2 : D is the translational diffusion constant and l the jump distance.

		D (10^{-5} cm 2 s $^{-1}$)	l (\AA)
270 K	AT2	0.2 ± 0.1	0.3 ± 2.9
300 K	AT1	2.43 ± 0.04	1.2 ± 0.2
	AT2	0.8 ± 0.1	1.1 ± 0.2
	AT3	0.25 ± 0.06	1.5 ± 0.3
	AT2-AT1	0.44 ± 0.04	0.9 ± 0.1
	AT3-AT1	0.20 ± 0.05	1.3 ± 0.3
330 K	AT2	0.9 ± 0.1	0.73 ± 0.02

CONCLUSIONS

Our SANS measurements confirm the absence of both sugar clustering and matrix deformation of the gels and indicate that the results presented in this work are representative of homogeneous trehalose solutions confined in a uniform matrix with an approximate pore size of 18 nm. Indeed, the optical clarity in conjunction with the SANS data constitutes a highly persuasive evidence for absence of phase separation. Our QENS results show that, while trehalose molecules are twice the size of D-glucose molecules, a confinement of 18 nm, mimicking the length scale in membranes, is still insufficient to significantly modify the translational dynamics. Trehalose molecules must be confined in smaller pores for the dynamics to be significantly affected. Mesoporous materials, particularly MCM-41-type silica nanospheres,²¹ appear as good candidates for investigating this possibility by QENS (Ref. 22) because of their exceptional regularity and small pore sizes.

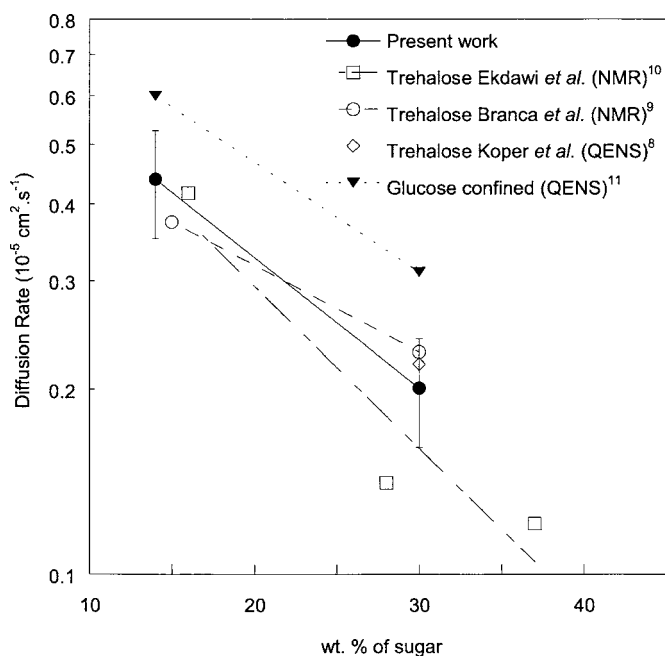


FIG. 7. Values of the diffusion constant for confined glucose (Ref. 11) (\blacktriangledown) and confined trehalose at 300 K in D_2O solutions from present work (\bullet) and experimental papers in the literature [\square : Ekdawi *et al.* (Ref. 10), \circ : Branca *et al.* (Ref. 9), \diamond : Köper *et al.* (Ref. 8)]. The lines represent a guide for the eye except for the values of Ekdawi *et al.*, where a least-squares fit has been made.

ACKNOWLEDGMENTS

This work was supported by the Centre National de la Recherche Scientifique, France and the U.S. National Institutes of Health. One of the authors (G.L.) acknowledges the Region Centre for a SOLEIL scholarship. The advice and encouragement of Dr. F. Fernandez-Alonso, Dr. S. Kline, Dr. W. S. Howells, Dr. L. Porcar, Dr. J. Teixeira, and Dr. J.-M. Zanotti are gratefully acknowledged, as well as the support of the ISIS and NCNR technical staffs.

- ¹P. Scott, *Ann. Bot. (London)* **85**, 159 (2000).
- ²J. H. Crowe, J. F. Carpenter, and L. M. Crowe, *Annu. Rev. Physiol.* **60**, 73 (1998).
- ³A. K. Sum, R. Faller, and J. J. de Pablo, *Biophys. J.* **85**, 2830 (2003).
- ⁴A. Patist and H. Zuerb, *Colloids Surf., B* **40**, 107 (2005).
- ⁵D. P. Miller and J. J. de Pablo, *J. Phys. Chem. B* **104**, 8876 (2000).
- ⁶J. Wolfe and G. Bryant, *Cryobiology* **39**, 103 (1999).
- ⁷J. L. Green and C. A. Angell, *J. Phys. Chem.* **93**, 2880 (1989).
- ⁸I. Köper, M.-C. Bellissent-Funel, and W. Petry, *J. Chem. Phys.* **122**, 014514 (2005).
- ⁹C. Branca, S. Magazù, G. Maisano, P. Migliardo, and E. Tettamanti, *J. Mol. Struct.* **480–481**, 133 (1999).
- ¹⁰N. Ekdawi-Sever, J. J. de Pablo, E. Feick, and E. von Meerwall, *J. Phys. Chem. A* **107**, 936 (2003).
- ¹¹G. Lelong, D. L. Price, A. Douy, S. Kline, J. W. Brady, and M.-L. Saboungi, *J. Chem. Phys.* **122**, 164504 (2005).
- ¹²L. J. Smith, D. L. Price, Z. Chowdhuri, J. W. Brady, and M.-L. Saboungi, *J. Chem. Phys.* **120**, 3527 (2004).
- ¹³C. Talò, L. J. Smith, J. W. Brady, B. A. Lewis, J. R. D. Copley, D. L. Price, and M.-L. Saboungi, *J. Phys. Chem. B* **108**, 5120 (2004).
- ¹⁴I. Jaymes, A. Douy, D. Massiot, and J.-P. Busnel, *J. Am. Ceram. Soc.* **78**, 2648 (1995).
- ¹⁵C. J. Glinka, J. Barker, B. Hammouda, S. Krueger, J. Moyer, and W. Orts, *J. Appl. Crystallogr.* **31**, 430 (1998).
- ¹⁶S. R. Kline, *J. Appl. Crystallogr.* **39**, 895 (2006).
- ¹⁷M. A. Adams, W. S. Howells, and M. T. F. Telling, Rutherford Appleton Laboratory Technical Report No. RAL-TR-2001-002, 2001 (unpublished).
- ¹⁸M. T. F. Telling and W. S. Howells, *GUIDE-IRIS Data Analysis* (ISIS Facility, Rutherford Appleton Laboratory, Chilton, Oxon, UK, 2000); W. S. Howells, *MODES Manual* (ISIS Facility, Rutherford Appleton Laboratory, Chilton, Oxon, UK, 2003).
- ¹⁹D. W. Schaefer and K. D. Keefer, in *Better Ceramics Through Chemistry*, edited by C. J. Brinker, D. E. Clark, and D. R. Ulrich (Elsevier North-Holland, New York, 1984).
- ²⁰J. Teixeira, M. C. Bellissent-Funel, S.-H. Chen, and A. J. Dianoux, *Phys. Rev. A* **31**, 1913 (1985).
- ²¹S. Bhattacharyya, G. Lelong, and M.-L. Saboungi, *J. Exp. Nanosci.* **1**, 375 (2006).
- ²²D. L. Price, M.-L. Saboungi, and F. J. Bermejo, *Rep. Prog. Phys.* **66**, 407 (2003).